

Input Impedance Spectrum for a Tenor Sax and a B_b Trumpet

David Pignotti

Department of Physics, University of Illinois, Urbana-Champaign

Chris Van de Riet

Department of Physics, University of Missouri—Rolla

Abstract

The input impedance spectrum of a reed-driven instrument gives information on which notes an instrument can produce and the relative difficulty a player encounters when playing a specific note. To measure the input impedance spectrum we used a piezoelectric transducer to excite the air within the instrument, the world's smallest microphone to measure pressure, and a custom-built differential pressure microphone to measure air particle velocity. Using these same components we developed a method of measuring not only the input impedance, but the sound intensity of any vibrating air column as well as free air.

I. Introduction

There are two different types of wind instruments, those that exhibit low or high input impedance at the point at which a player excites the air flowing through the instrument. The low-impedance group refers to instruments such as the flute, organ pipe, or recorder. We are interested in measuring the input impedance of the high impedance group—reed driven instruments (be they wooden reeds or lip reeds) such as the clarinet, saxophone, or trumpet.¹ For our experiment we will focus specifically on the input impedance of a trumpet and a tenor saxophone, but our method can easily be applied to any musical instrument, as well as for any arbitrary sound field.

When a player's lips excite the air that is forced through a trumpet, the air resonates at the natural frequency of the tube in which the air flows. In the case of the trumpet the tube appears to be open—It is open at the mouthpiece and open at the bell. Thus, one would expect the trumpet to produce the fundamental frequency associated with the ~147 cm tube length ($f_0 \approx 117$ Hz, C₃) and all the subsequent even and odd harmonics (C₄, G₄, C₅, E₅, G₅, a flat B_{b5} and C₆) when no valves are pressed.² This model agrees with the notes that can actually be played when all 3 of the valves of the trumpet are up. However, even though the tubing of a trumpet is open, there is such a large impedance mismatch at the bell end of the trumpet that the tubing is effectively closed at the bell end. As a result, a trumpet will produce a

fundamental frequency that is a factor of two times lower than the open-tube model ($f_0 \approx 58.5$ Hz) and only the odd harmonics will be present.² How does the trumpet overcome this problem?

By measuring the acoustical input impedance spectrum we can see how the frequencies that should be produced by a trumpet are shifted to the frequencies that are observed.

The saxophone is a woodwind instrument, and therefore operates in a somewhat different manner than the trumpet. The vibrations of the air column are created by a cane reed, which is clamped to the mouthpiece at one end with a metal ligature. The reed receives feedback from the reflected pressure waves regarding the proper vibrational frequency needed to excite a resonance of the instrument. Unlike the trumpet, where one valve combination is used to play many notes, the saxophone has a different key combination for each note - the player closes keys which become subsequently closer to the bell of the instrument in order to play subsequently lower-frequency notes.

The saxophone family consists of various members which vary mainly by their physical size (and consequently, their available frequency ranges); the middle-sized tenor saxophone, pitched in B_b , is examined in this experiment.

Even though the saxophone has a conical bore, it can be roughly approximated as an open-open cylindrical tube, and therefore excites both even and odd harmonics, with the lowest available frequency for the tenor saxophone (given an overall length of 1.4 m) being concert-pitch A_{b2} at 103.83 Hz.

II. Background

Acoustical input impedance is defined as a measure of resistance to putting a pressure wave through a tube.³ The quotient of the complex pressure wave inside the instrument and the complex air particle velocity gives the value of the complex impedance:

$$\tilde{Z}(r) = \frac{\tilde{P}(r)}{\tilde{U}(r)}$$

The SI units of impedance are $\text{Pa}\cdot\text{s}/\text{m}$ ($= \text{kg}/\text{m}^2\cdot\text{s}$) or simply “acoustical ohms.” When a trumpet is played, the player’s lips vibrate, injecting bursts of air and pressure into the trumpet tubing. The pressure wave travels through the trumpet and is reflected back towards the mouthpiece when it encounters a sharp change of the radius of the tube at the bell end of the trumpet. The reflected pressure wave gives the player’s lips “information” on the frequency at which to vibrate. Therefore, the higher the impedance, the greater amount of pressure waves reflected, and thus the easier it is to play that note.³ This phenomenon allows the trumpet to sound a desired note with ease.

Backus investigated the change in the input impedance spectrum throughout the various stages of the construction of a trumpet. The lowest mode is actually the second harmonic since the fundamental frequency for brass instruments cannot be used. Due to the construction of the mouthpiece which caters to the higher harmonics, the fundamental frequency is only available to extremely experienced players. Nevertheless, the trumpet is driven by the player’s lips at the fundamental frequency, thus higher harmonics appear at integer multiples of the fundamental.

Figure 1 shows the input impedance peaks for the construction of a trumpet. The cylindrical tubing alone shows a steady decrease in the magnitude of the input impedance peaks as frequency increases, but the peaks do not line up with the desired note frequencies for a trumpet. When the bell is added, the input impedance peaks still steadily decrease but the higher modes decrease more rapidly than they did without the bell. The bell also matches the input impedance peaks with desired the frequencies better than with just the tubing. The tubing plus mouthpiece and leader pipe show a steady increase of the input impedance peaks of the modes as frequency increases and then displays a sharp falloff after about the 8th harmonic. The input impedance peaks are

somewhat better matched to the desired frequencies. When the bell is added to this 3rd system, the input impedance peaks shift to almost exactly the frequencies required for a trumpet.⁴

Figure 2 shows the discrepancies between the n^{th} resonance and the n^{th} harmonic throughout the stages of construction of a trumpet. Before the instrument is put together, the deviation from the resonances and the harmonics for just the cylindrical tubing at the 5th mode is 1/4 an octave. When the bell is added, the deviation at the 5th mode is 1/6 an octave. When the mouthpiece is added, the deviation is lowered to 1/12 of an octave. Finally, when the instrument is complete there is no appreciable deviation from desired harmonics.⁴

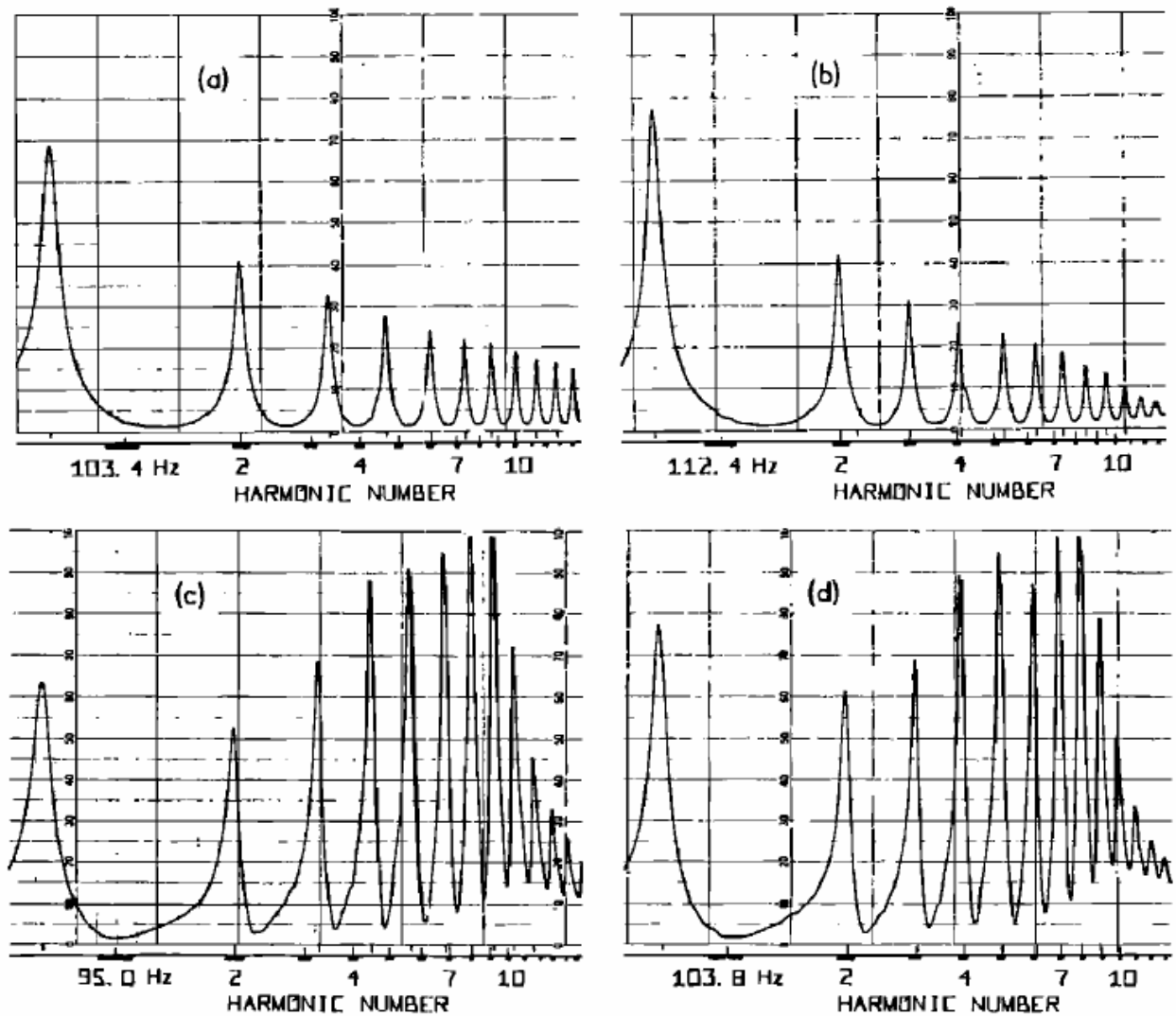


Figure 1. Input impedance curves for the construction of a modern Bb trumpet. (a) a length of cylindrical tubing; (b) tubing plus trumpet bell; (c) tubing plus mouthpiece and leader pipe; and (d) tubing plus bell plus mouthpiece and leader pipe. Full scale is 1000 acoustic Ω .⁴

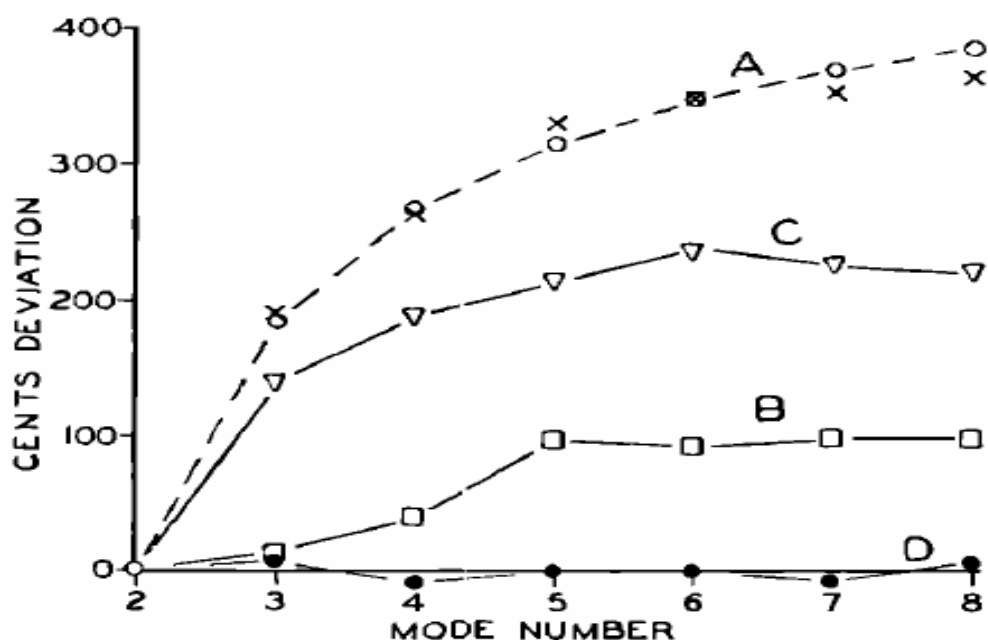


Figure 2. Plots of the discrepancies in cents between the n^{th} resonance and the n^{th} harmonic, with the second resonance coinciding with the second harmonic. (a) Cylindrical tubing; (b) tubing plus bell; (c) tubing plus leader pipe and mouthpiece; and (d) tubing plus bell plus leader pipe and mouthpiece.⁴

In order to measure the complex input impedance of an instrument Benade developed a piezo-disk-driven impedance head apparatus.⁵ This technique involves attaching a piezo-transducer onto the mouthpiece of the instrument. Benade states that if the stiffness of the piezoelectric disk is large compared to the highest possible input impedance of the air column under study, then the acoustical pressure observed at the input end of the air column is an accurate measure of the air column's own input impedance. He further states that this measurement of the air column's input impedance is accurate as long as the frequency at which the tube is excited is not a resonant frequency of the piezo-transducer. A microphone is then inserted into the mouthpiece near the

piezo-transducer. Benade used the microphone to measure the pressure response to the voltage-dependent oscillations provided by the transducer. He states that his microphone has a flat frequency response from 50 Hz to 5000 Hz. The air particle velocity, Benade claims, is related to the amount of air displaced by the piezo transducer. Using these two values of pressure and air particle velocity the acoustical impedance could easily be calculated over a range of frequency.⁵ We can improve upon the piezo-transducer method by directly measuring the air particle velocity using a differential pressure microphone.

III. Experimental Apparatus

We measured the acoustic input impedance using a piezoelectric driver, two 1/10" Knowles Acoustics FG-23329 high performance omni-directional microphones to measure pressure, and two modified RadioShack 270-090 condenser microphones to measure particle velocity. A pressure microphone and a particle velocity microphone were secured inside the mouthpiece near the piezo-transducer to determine the input impedance. The remaining two microphones were placed outside the mouthpiece in proximity to the transducer (Figure 3). The external microphones are used to detect potential coupling of the internal pressure and particle velocity of the instrument with the free air.

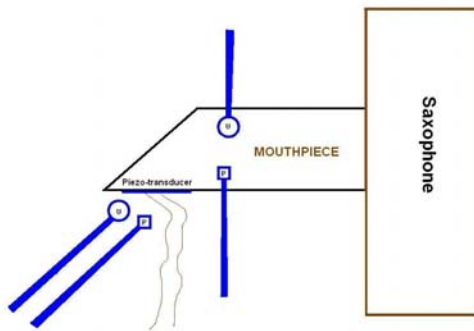


Figure 3. The particle velocity microphone, U , and the pressure microphone, P , are secured inside the mouthpiece. The remaining microphones are located outside the mouthpiece, in proximity to the transducer, and are used to detect relationships between internal and external pressure and particle velocity.

The Knowles Acoustics omni-directional microphone used to measure the pressure is 0.1" in diameter which makes it the smallest microphone in the

world.⁶ This microphone was chosen because of its small size and its flat frequency response up to 10,000 Hz (Figure 4). Keeping the components inside the instrument's mouthpiece as small as possible is important so as to minimally disturb the air volume of the mouthpiece to ensure negligible disruption of airflow. The Knowles Acoustics microphones were each connected to custom built preamps (Figure 5) to increase the voltage output from the microphone before being fed into lock-in amplifiers. Plots of the voltage gain vs. frequency and the phase vs. frequency of the Knowles Acoustics microphone preamplifiers are shown in Figure 6. The voltage gain of this preamp is flat up to 1.0 MHz while the phase stays constant up to 40.0 kHz, both of which are well over the audio frequency range.

The particle velocity microphones were made from modified RadioShack type 270-090 electret condensor microphones. The design of the modification of this microphone was introduced by Bennet-Clark in his paper concerning the measurement of air particle velocity produced by small insects.⁷ The modified microphone components are a pressure gradient transducer, a FET impedance converter, and a fine copper mesh screen used for shielding the interior components of the microphone from exterior sources of electromagnetic noise. Once we have the differential pressure signal from the modified microphone, in order to obtain a voltage signal linearly proportional to the particle velocity we integrate the differential pressure signal over the time the instrument is being driven,

$$u(t) = (1/\rho_o d) \int_{-\infty}^t [p_1(t') - p_2(t')] dt'$$

where ρ_o is the ambient density of air and d is the separation distance between the acoustic centers of the differential microphone.⁸

This integration is accomplished by routing the signal from the particle velocity sensor through a custom-built integrating preamp (Figure 7) before being connected to the lock-in amplifier. The frequency response of the combined particle velocity microphone and

integrating amplifier is flat in the audio frequency range of interest (100→3000 Hz) and the phase response is constant to within 10° over this same frequency range. Plots of the voltage gain vs. frequency and the phase vs. frequency of the integrating preamplifier are shown in Figure 8. The voltage gain of the preamp decreases logarithmically with frequency whereas the differential microphone output increases logarithmically over this same frequency range from 10 Hz to 10 kHz.

The piezo-transducer that excites the air in the instrument is driven by a

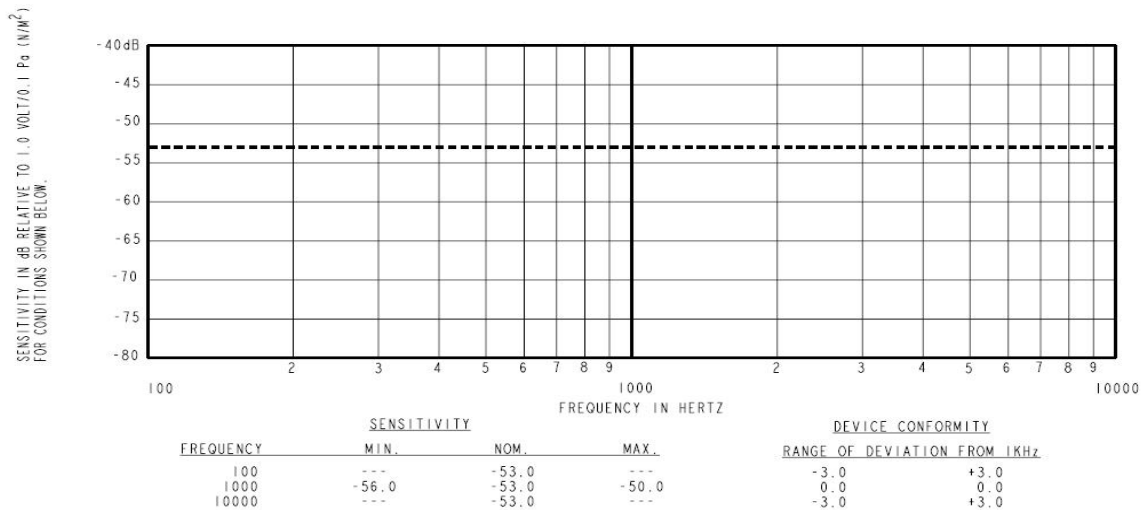


Figure 4. Frequency response of the 0.1 inch Knowles Acoustics FG-23329 microphone is flat up to 10,000 Hz.⁹

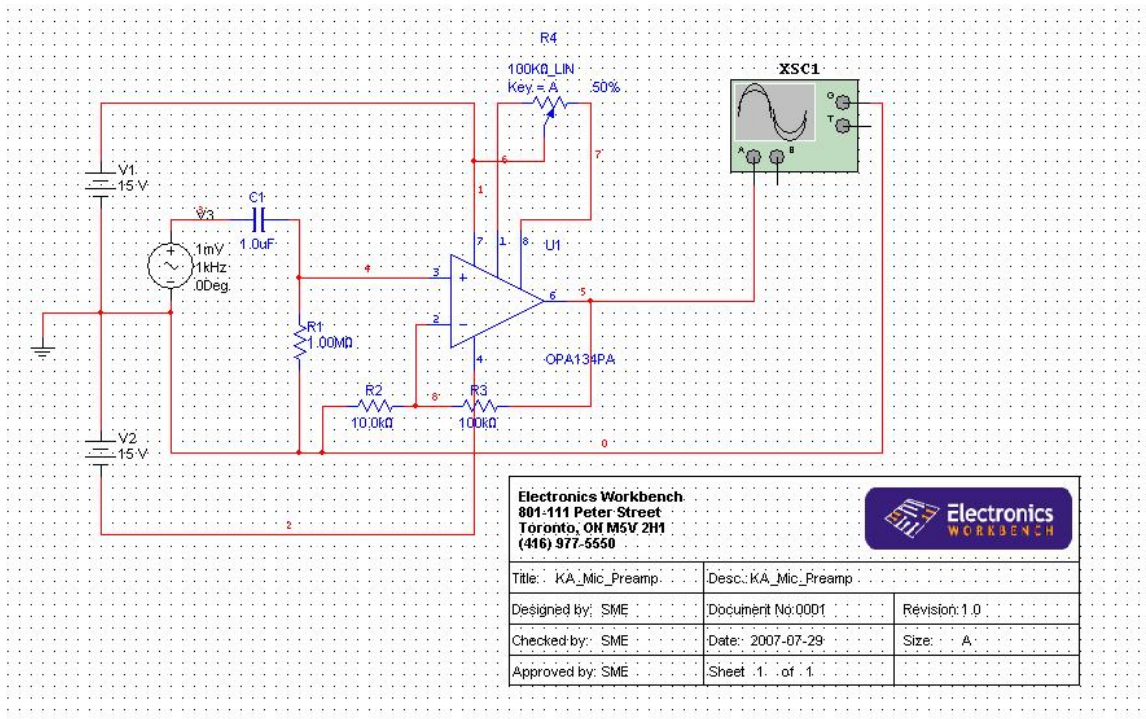


Figure 5. Schematic of the Knowles Acoustics microphone preamplifier. The OPA134PA op-amp amplifies the microphone voltage by a factor of 11x.

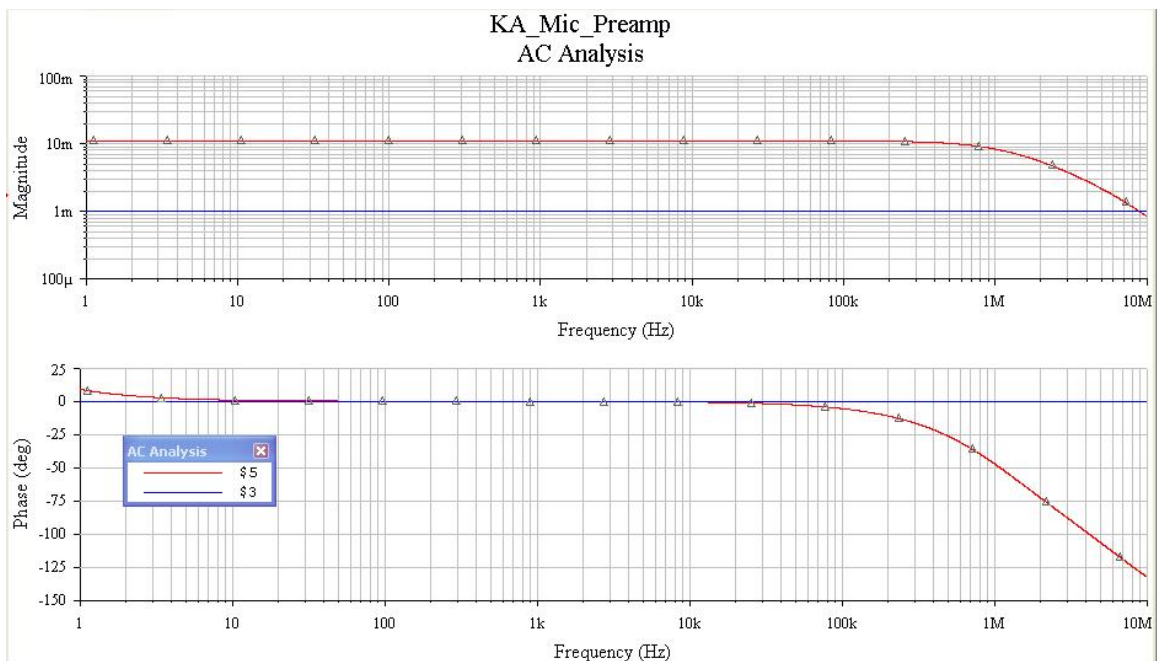


Figure 6. Voltage gain and phase plots of the pressure microphone preamplifiers on a logarithmic frequency scale. The red \$5 line represents the output of the preamplifiers.

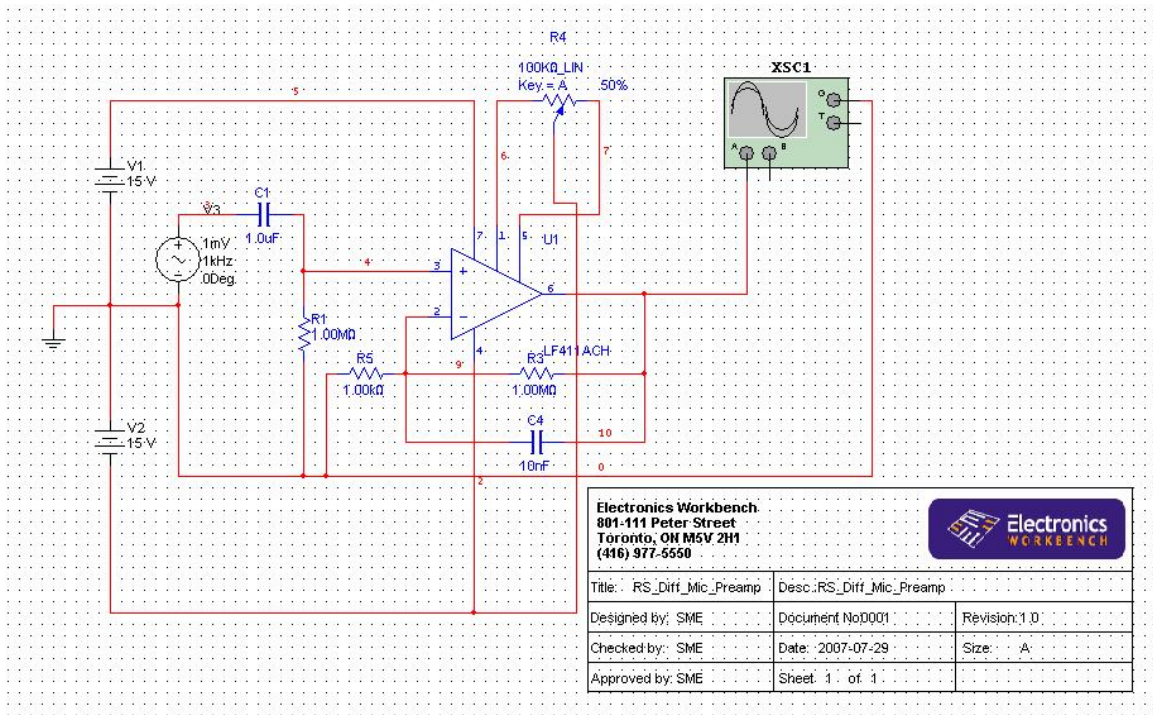


Figure 7. Integrating preamp circuit integrates the differential pressure signal from the particle velocity microphone when the instrument is being driven.

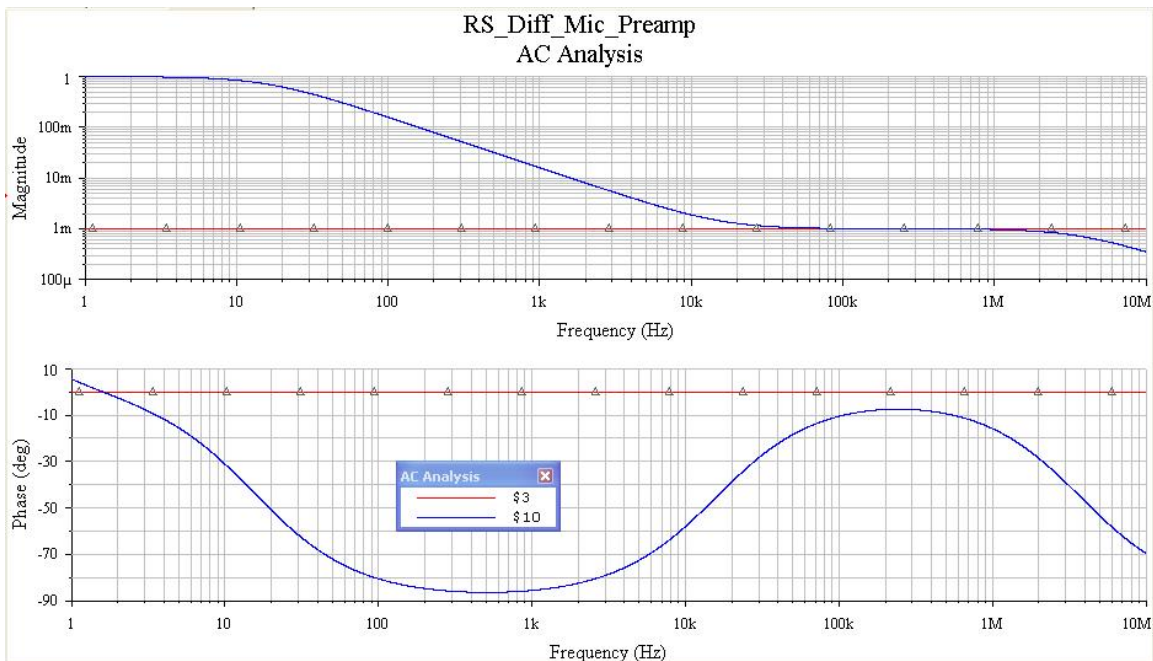


Figure 8. Voltage gain and phase plots of the differential pressure particle velocity microphone integrating preamplifiers on a logarithmic frequency scale. The blue \$10 line represents the output of the preamplifiers.

computer controlled Agilent 33220A function generator. The driving voltage passes through a custom built voltage amplifier (Figure 9) to boost the output voltage. Plots of the voltage gain vs. frequency and the phase vs. frequency of the voltage amplifier are shown in Figure 10. The driving voltage then passes through a negative impedance converter (NIC) circuit (Figure 11) to provide the piezo-transducer with true constant current and a phase shift of 90° over the full range of interest in the audio frequency band. Plots of the voltage gain vs. frequency and the phase vs. frequency of NIC constant current driven circuit are shown in Figure 12.

Once the piezoelectric driver, microphones, and differential microphone particle velocity sensors have been assembled and installed inside and outside the mouthpiece, the apparatus is then connected up to a modified version of the UIUC Physics 498POM PC-Based Electric Guitar Pickup/ Loudspeaker Impedance Measuring System shown below in Figure 13. This PC-Based DAQ System was developed to measure the electrical impedance of electric guitar pickups and loudspeakers. An interesting aspect of complex acoustical impedance ($\tilde{Z}_{\text{acoustic}}$) is that it can be related to complex electrical impedance ($\tilde{Z}_{\text{electric}}$):

$$\tilde{Z}(r)_{\text{acoustic}} = \frac{\tilde{p}(r)}{\tilde{U}(r)} \quad \text{and} \quad \tilde{Z}_{\text{electric}} = \frac{\tilde{V}}{\tilde{I}},$$

where complex the pressure (\tilde{p}) is the analogue of complex voltage (\tilde{V}) and the complex air flow (\tilde{U}) is the analogue of complex electric current (\tilde{I}). Therefore connecting our trumpet/sensors to the Electric Guitar

Pickup/Loudspeaker Impedance Measuring System is completely straightforward.

Our modified system uses a computer-controlled sinusoidal function generator to set the frequency and amplitude of the piezo-driver as used in the previous system. The voltage signals produced by the microphones and the air particle velocity sensors are individually fed into four SRS-830 DSP lock-in amplifiers, using the piezo-driver voltage signal as a reference in order to determine phase information. The real and imaginary parts of both the microphone voltages and the u-sensor voltages are digitized using eight ADC channels on a National Instruments LabPC+ DAQ Card and stored in arrays.¹⁰

The computer starts the piezo-driver oscillating at a user-defined frequency and amplitude. Once the pressure microphone and u-sensor voltage data has been digitized (10,000x per frequency point) and stored, the PC increases the piezo-driver frequency by a user-defined step size and the process is repeated. The driving frequency can thus be swept over the entire audio frequency range (20 Hz \rightarrow 20,000 Hz). For the purposes of trumpet and saxophone input impedance measurements, we ran frequency sweeps from 20 Hz to 4020 Hz with a 1 Hz step size for high resolution plots. The air in the tubing coupling to higher-order vibrational modes other than the longitudinal mode at frequencies higher than 3000 Hz limits the usefulness of performing frequency scans up to 20,000 Hz. Each run of the program took approximately three to five hours since there was a 5 second wait for the lock-in amplifiers to settle/frequency point. Once the DAQ

program has been run the results can be plotted on 21+ separate on-line graphs (Re(Z) vs. f, Re(I) vs. f, Re(P) vs. f,

Re(U) vs. f, etc...) and the data file is written out to a file for offline analysis.¹⁰

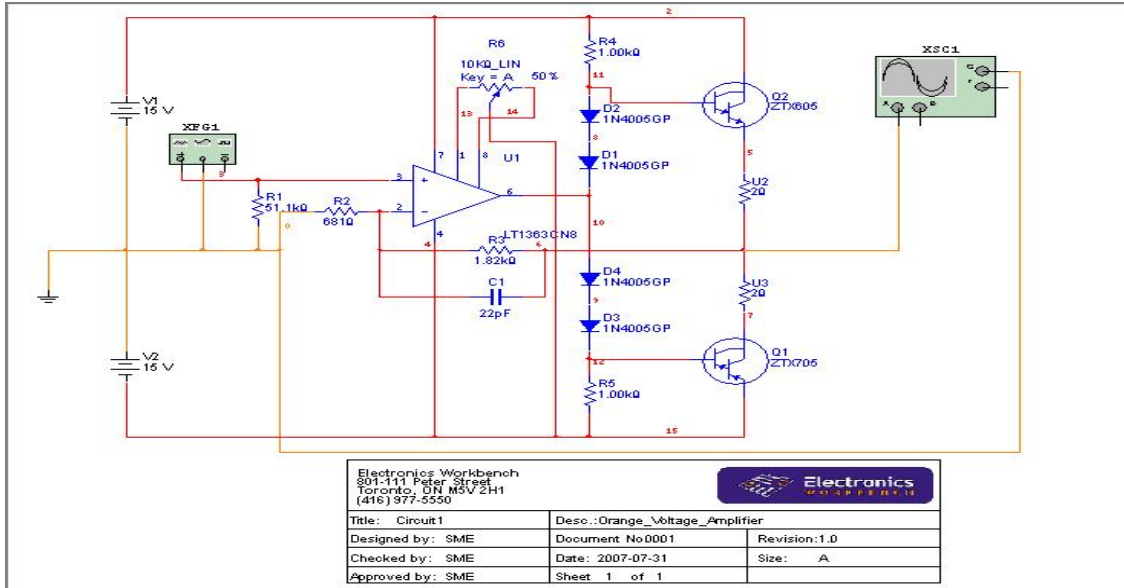


Figure 9. The voltage amplifier increases the voltage output from the function generator to the piezo-transducer resulting in a 3x increase in amplitude relative to that where the transducer was driven with the function generator alone.

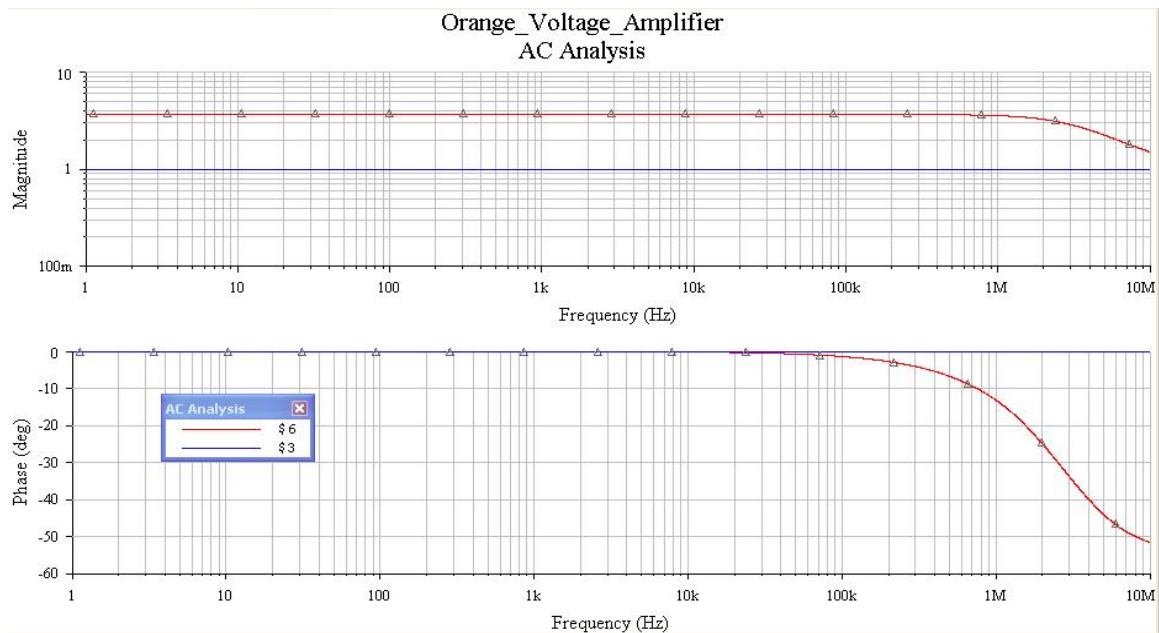


Figure 10. Voltage gain and phase plots of the voltage amplifier on a logarithmic frequency scale. The red \$6 line represents the output of the preamplifier.

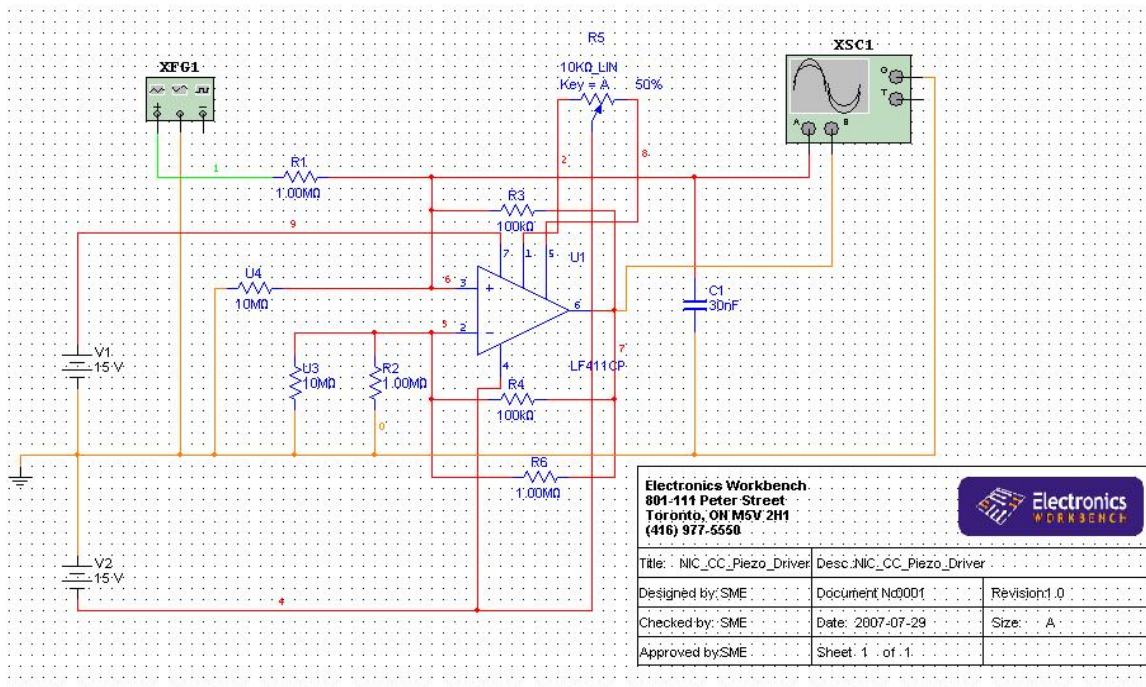


Figure 11. The NIC constant-current piezo-driver circuit provides a $\sim 0.91\text{M}\Omega$ negative resistance which nearly completely cancels the $1.0\text{M}\Omega$ coupling resistance. The cancellation of the coupling resistance allows the function generator/voltage amplifier to act as an near-ideal current generator.

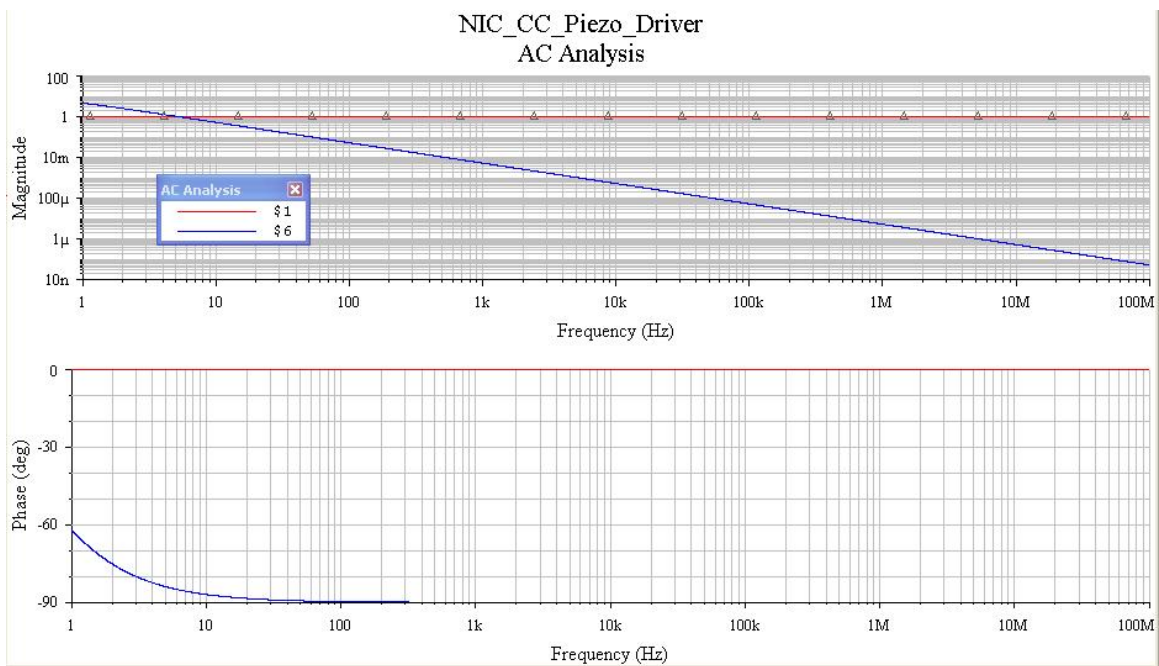


Figure 12. Voltage gain and phase plots of the NIC constant-current piezo-driver circuit on a logarithmic frequency scale. The blue \$6 line represents the output of the NIC constant-current piezo-driver circuit.

IV. Results and Discussion

As previously stated, we placed a pressure and particle velocity microphone outside the mouthpiece in order to determine if interior vibrations were affecting the air outside the instrument. The raw pressure and particle velocity data both inside and outside the mouthpiece are plotted in Figure 14. The external microphones showed little relation to the internal microphones. This result explicitly confirms the decoupling of the air vibrations as being due to the piezo-transducer's stiffness, thereby not allowing internal vibrations to affect external vibrations.

Due to the size of our particle velocity microphone, we could not fit it in the mouthpiece of the trumpet without severely disrupting airflow. Therefore, currently we are unable to obtain particle velocity data for the trumpet. The bore of the tenor sax's mouthpiece is much larger than that of the trumpet which makes placement of the particle velocity

microphone in the mouthpiece feasible. A plot of the tenor sax's particle velocity vs. frequency with all tone holes closed is shown below in Figure 15.

A comparison between the pressure for the tenor sax and the B $_b$ trumpet is shown below in Figure 16. The first pressure peak for the trumpet and the saxophone agree quite well. As the frequency increases, the frequencies at which the pressure peaks occur become increasingly high compared to the known allowed frequencies of the Dn-Up-Up valve configuration. Since the pressure data is only half of the impedance equation, when the particle velocity data is obtained and combined with the pressure data, the frequencies of the impedance peaks of the trumpet will closely match those of known allowed frequencies.

Even though the early particle velocity peaks for the saxophone are hampered by 1/f ventilation noise up to 200 Hz, the frequencies at which the pressure maxima and particle velocity minima occur agree to within a few Hz.

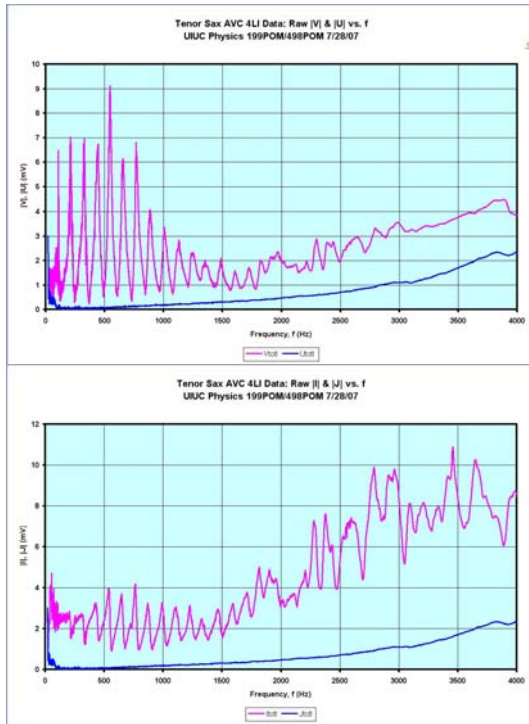


Figure 14. Raw pressure (top) and particle velocity data (bottom). The smooth lower line on each plot represents data taken with the exterior microphones. The peaks measured with the interior microphones are not detected by the exterior microphones.

The quotient of the input pressure and input particle velocity gives input impedance, Z , vs. frequency for the tenor saxophone shown below in Figure 17. The input impedance spectrum, as stated earlier, gives information on which notes are allowed for an instrument and the relative ease for playing a specific note. Unlike brass instruments, the tenor saxophone and all woodwind instruments are designed to play one note per key combination. This difference makes the most important peak for woodwinds the first, fundamental peak. The subsequent peaks, while representing possible available notes, fulfill the task of enriching the saxophone's timbre. The

trumpet, which has far less valve combinations, needs all its impedance peaks to cover its musical scale. The fundamental impedance peak for the tenor saxophone with all tone holes closed occurs at ~ 108 Hz. This frequency closely matches the accepted note frequency of 103.83 Hz. The sharpness of pitch of our experimental result can easily be attributed to the saxophone being slightly out of tune.*

An interesting result of the combination of particle velocity and pressure to obtain input impedance is the symmetry of the input impedance peaks. When examining the particle velocity data we noted a relatively gradual rise of particle velocity with frequency until a peak was reached at which point the particle velocity experienced a sharp drop before gradually rising to the next peak. This pattern of gradual rises and sharp falls with increasing frequency is reversed in the pressure plot which experiences a sharp rise and a gradual fall with increasing frequency. Thus, when input impedance $Z = P/U$ is plotted, the peaks experience symmetrical sharp rises and falls. The fact that it is just as easy to play a note sharp as it is to play the same note flat is attributed to this phenomenon.

* Tuning is determined by the insertion depth of the mouthpiece onto the neck of the saxophone.

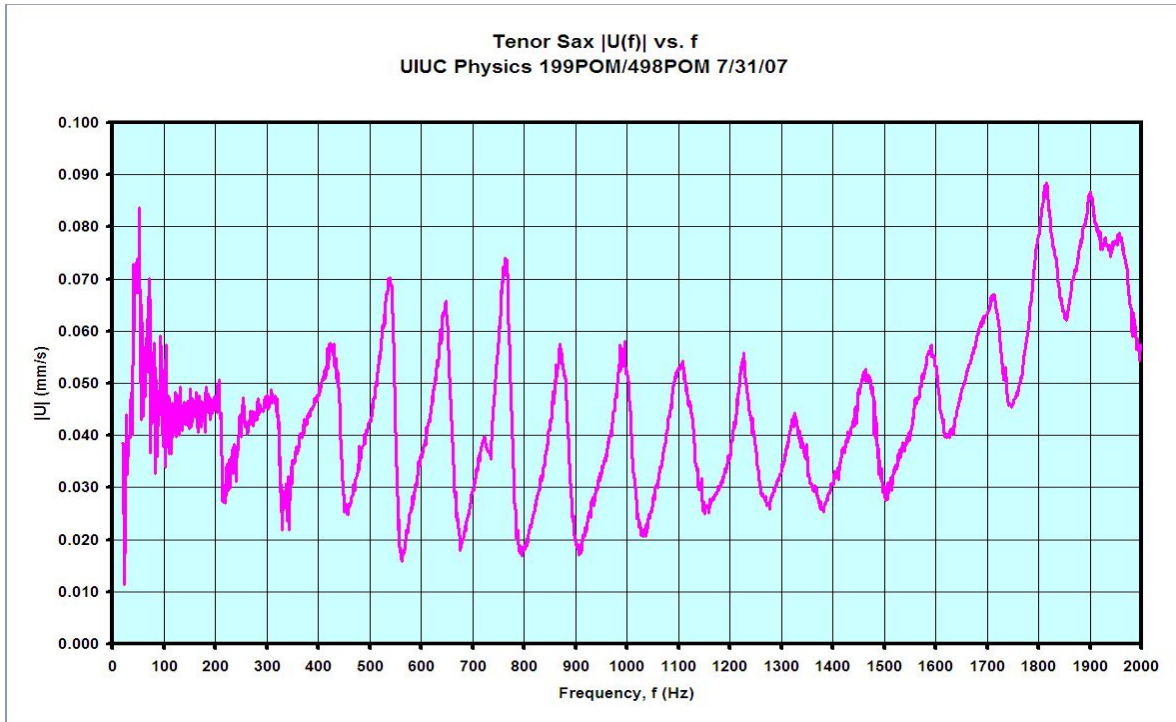


Figure 15. Particle velocity spectrum (in mm/s) of the tenor saxophone with all the tone holes closed up to a frequency of 2000 Hz. The peaks and dips below 200 Hz are hampered by $1/f$ noise from the ventilation system in the room where the experiment was carried out.

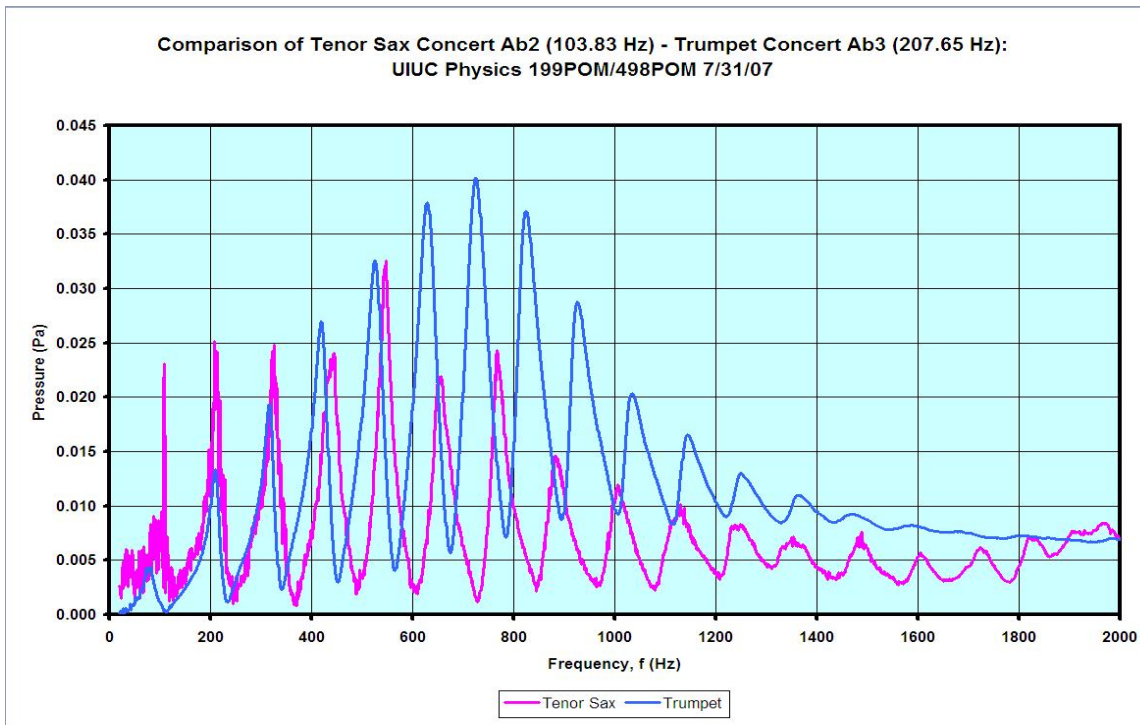


Figure 16. Comparison of pressure data between trumpet and tenor saxophone. Peak positions agree for low frequencies, but alignment becomes worse and worse as frequency increases.

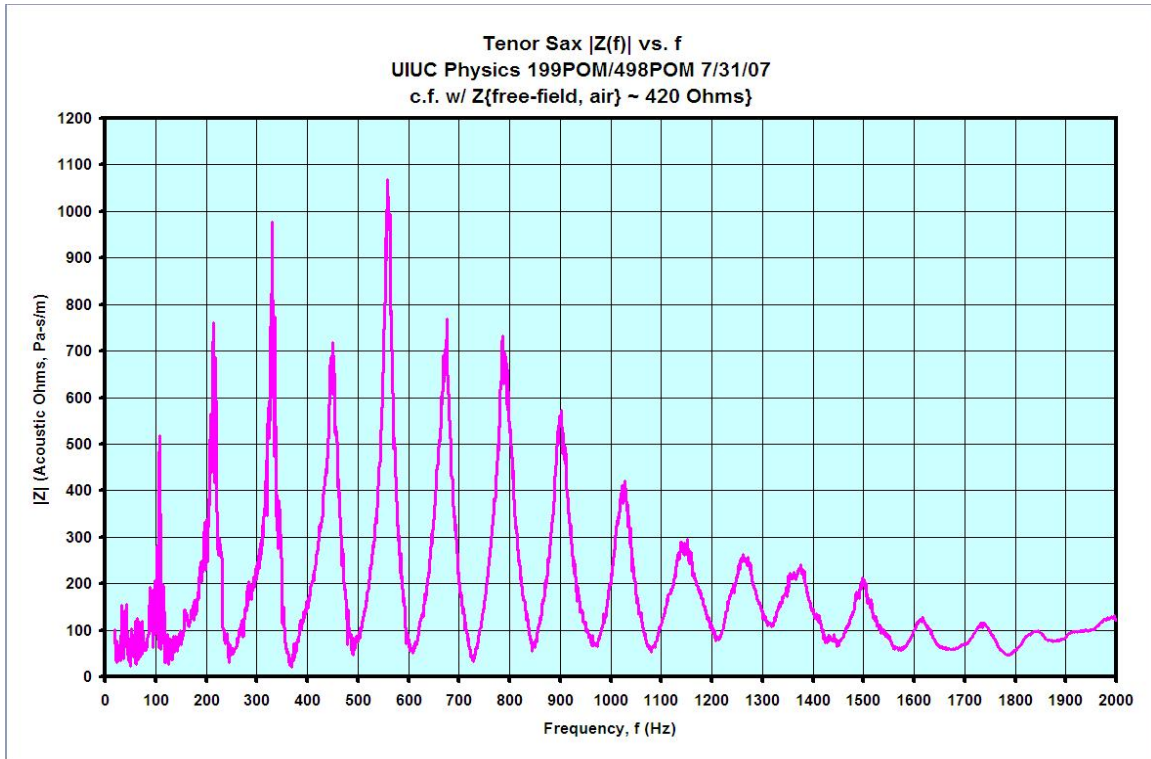


Figure 17. Tenor saxophone input impedance peaks (all tone holes closed) over a range of frequency up to 2000 Hz. The first peak at ~108 Hz closely matches the ~104 Hz concert $A\flat_2$ the tenor sax was designed to play with all the tone holes closed.

We initially set out to determine the input impedance of a musical reed-driven instrument, however, using the same pressure and air particle velocity data, we can additionally determine the longitudinal component of the complex

{vector} sound intensity (in Watts/m²) at the input point (see Figure 18):

$$\tilde{\mathbf{I}}(\mathbf{r}) = \tilde{\mathbf{P}}(\mathbf{r}) \cdot \tilde{\mathbf{U}}(\mathbf{r}).$$

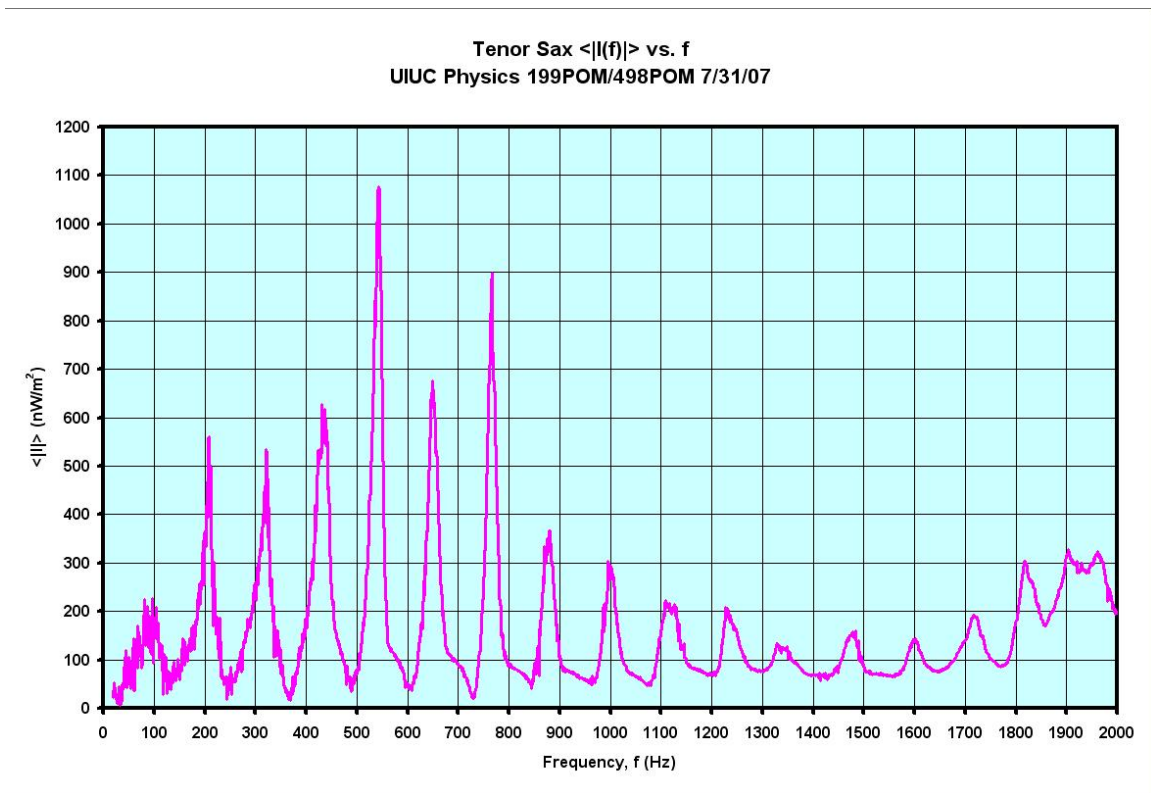


Figure 18. The time-averaged longitudinal component of the acoustical input intensity of the tenor saxophone over a range of frequencies up to 2000 Hz.

V. Future Work

The process described above produces the input impedance spectrum for one key combination of the saxophone. Since we have a working apparatus to measure one key combination, we can apply our technique to different key combinations in an attempt to measure the effect the keys themselves have on the impedance spectrum. We would also like to complete further analysis of complex phase data.

While this paper primarily focused on the trumpet and the saxophone, using a pressure sensitive microphone and our developed particle velocity sensor enables us to measure the complex

acoustical impedance of any instrument or vibrating column of air. We can also use the sensor combination to obtain the acoustical impedance of free space or an arbitrary sound field

Miniaturization of the differential pressure system for measuring particle velocity would be extremely useful. As stated earlier, the kinds of instruments that we can determine the input impedance and sound intensity is currently restricted by our relatively large differential pressure microphone. Instead of using one large differential microphone, it is also possible to use two Knowles Acoustics microphones in proximity to each other with a specific geometrical configuration (face-to-face, side-by-side, tandem, or back-to-back)⁸.

A smaller particle velocity microphone will have less impact on the air flow in the mouthpiece of any instrument.

While the integral of the differential pressure signal from the differential microphone yields a signal linearly proportional to the particle velocity, we would like to do better by measuring the particle velocity directly. We currently have prototypes for several candidate particle velocity sensors that have the potential of directly measuring air particle velocity.

VI. Acknowledgements

We thank Prof. Steven Errede and Mr. Jack Boparai for their continuing help with this research.

We also thank the University of Illinois Physics Department and the National Science Foundation for their support.

VII. References

¹J. Backus, J. Acoust. Soc. Am. 54, 470 (1974).

²J. Jeans, “The Vibrations of Air,” in Science & Music (Dover Publications, New York, 1968), Ch. IV, pp. 107–151.

³J. Backus, J. Acoust. Soc. Am. 60, 1266 (1976).

⁴T. Moore, International Trumpet Guild Journal 27, 70 (2002).

⁵A.H. Benade, J. Acoust. Soc. Am. 81, 1152 (1987).

⁶Knowles Acoustics, High performance microphones FG series, http://www.knowlesacoustics.com/knowlesacoustics-apps/specialty_productdetail.do?product_id=7 (August 1, 2007)

⁷H.C. Bennet-Clark, J Exp Biol. 108, 459-463 (1984)

⁸F.J. Fahy, “Principles of measurement of sound intensity,” in Sound Intensity (St Edmundsbury Press, Suffolk, 1989), Ch. 5, pp. 89–107.

⁹Knowles Electronics, FG-23329-C05 datasheet, <http://www.knowlesacoustics.com/images/specs/FG-23329-C05.pdf> (August 3, 2007)

¹⁰S. Errede, presented at the Audio Engineering Society, University of Illinois at Urbana-Champaign, Nov 9, 2005 (unpublished). http://online.physics.uiuc.edu/courses/phys498pom/Lecture_Notes/Guitar_Pickup_Talk/Electronic_Transducers_for_Musical_Instruments.pdf (August 1, 2007)